Construction and Building Materials 172 (2018) 608–617

Contents lists available at ScienceDirect

Construction and Building Materials

journal homepage: www.elsevier.com/locate/conbuildmat

Improving shear strength of beams using ferrocement composite

Taha A. El-Sayed *, Abeer M. Erfan

Department of Civil Engineering, Shoubra Faculty of Engineering, Benha University, 108 Shoubra St., Shoubra, Cairo, Egypt

HIGHLIGHTS

- Shear behavior of beams reinforced by ferrocement.
- Shear behavior were studied in experimental & analytical manners.
- Nonlinear finite element analysis was performed using Ansys 14.5.

ARTICLE INFO

Article history:
Received 14 December 2017
Received in revised form 27 March 2018
Accepted 30 March 2018

Keywords:
Ferrocement
Welded wire mesh
Expanded wire mesh
Nonlinear finite element analysis (NLFEA)
Ansys 14.5

ABSTRACT

The Paper opens up a new issue of shear behavior of beams reinforced by ferrocement. The significant parameters utilized were shear reinforcement, stirrups and wire meshes. The replacement of wire mesh occurred in respect of the weight with stirrups. The influence of ferrocement was studied using the experimental inspection, and results of nonlinear finite element analysis. The experimental program includes seven (7) beams were tested using two-point loading system. Beams with welded wire mesh exhibited some amount of increase in shear capacity in respect of beams with reference & expanded wire mesh. Nonlinear finite element analysis was performed using Ansys 14.5. The analytical results demonstrated good consistent with the experimental results. Also, beams with wire mesh showed less number of crack patterns compared to the reference.

1. Introduction

Many researchers have been conducted on the ferrocement as a low cost construction material and a flexible structural system, and many parameters were carried out to validate the new system and to enhance its performance [1,2].

Al-Sulaimani et al. [3] carried out an experiment of flanged beams to study shear behavior of ferrocement. The results indicated that cracking and ultimate shear strength increased as wire mesh in webs is increased and as the shear span to beam depth ratio (a/h) is decreased.

Mansur et al. [4] studied the shear behavior of ferrocement beams. The results indicated that the ultimate shear strength increased as the shear span to beam depth ratio (a/h) is decreased and ferrocement Volume of fraction (Vt) and mortar strength (fcu) are increased.

Fahmy et al. [5] conducted a research on the ferrocement panels for use as floor units. In their study, they developed ferrocement sandwich panels and hollow core panels to be investigated as flexural slabs. The results showed that ferrocement hollow core panels yielded higher ultimate loads than the ferrocement sandwich panels. The weight of the proposed panels is about 67% of the weight of an equal reinforced concrete panels.

Walker et al. [6] considered the viability of using an external ferrocement coating to provide the shear strengthening. Results of preliminary experimental investigation, undertaken to assess the use of ferrocement for shear reinforcement. For both masonry and grouted cavity construction the shear span/effective depth ratio (a/d) has a major influence on performance. For low (a/d) ratios, the beam reacts as a tied arch. The shear strength of reinforced brickwork is less than both equivalent reinforced concrete and grouted cavity sections.

Basunbul et al. [7] studied the structural performance of ferrocement sandwich load bearing wall panels. Test results showed that ferrocement wall panels reinforced with wire mesh only exhibited better lateral and axial ductility than panels that contained the same amount of wire mesh plus skeletal steel due to the delaminating effect and buckling of skeletal steel.

2. Experimental program

The experimental study was performed in the laboratory at the Shoubra Faculty of Engineering, Benha University, Egypt. The main

* Corresponding author.
E-mail addresses: taha.ibrahim@feng.bu.edu.eg (T.A. El-Sayed), abir.arfan@feng.bu.edu.eg (A.M. Erfan).

https://doi.org/10.1016/j.conbuildmat.2018.03.273
0950-0618/

objective was studying the ultimate load, ultimate deflection, stiffness, toughness, shear stress, and mode of failure at collapse of the control beams, which were reinforced with steel and to contrast their performance with those common reinforced ferrocement beams reinforced with expanded wire mesh and welded wire mesh.

2.1. Experimental study: materials used are

1. Fine aggregate: was of natural siliceous sand with a modulus of fineness 2.75.
2. Cement: Ordinary Portland type CEM I 42.5 N (El-Suez Cement Company).
3. Water: Tap water used for mixing and curing procedures.
4. Super plasticizer: with a density of 1.2 kg/litre and an amount of 1.0% of the cement weight.
5. Reinforcing steel: Two types of reinforcing steel obtained from El-Dekhiela factory: Type I: Normal mild steel 24/35 (plain bars), Type II: High grade steel 36/52 (deformed bars).
6. Reinforcing wire meshes: Fig. 1 showed expanded & welded wire mesh used as reinforcement for ferrocement. The mechanical properties of welded & welded wire mesh according to manufacturer are given in Table 1.

2.2. Mortar matrix

The concrete mortar was designed to get a compressive strength (f_{cu}) of 30 MPa at 28 days. Mix properties based on "ACI committee 549 [1] " are listed in Table 2.

a) Expanded wire mesh b) Welded wire mesh

Fig. 1. Types of meshes.

Table 1
Mechanical properties of expanded and welded wire mesh.

Expanded Wire Mesh		Welded Wire Mesh	
Dimensions size	16.5 × 31 mm	Dimensions size	12.5 × 12.5 mm
Weight	1660 gm/m^2	Weight	600 gm/m^2
Sheet Thickness	1.25 mm	Wire Diameter	0.7 mm
Young's Modulus	12000 N/mm^2	Young's Modulus	17000 N/mm^2
Yield Stress	250 N/mm^2	Yield Stress	400 N/mm^2
Yield Strain	9.7 × 10^{-3}	Yield Strain	1.17 × 10^{-3}
Ultimate Strength	380 N/mm^2	Yield Strain	600 N/mm^2
Ultimate Strain	59.2 × 10^{-3}	Ultimate Strain	58.8 × 10^{-3}

2.3. Samples description

The experimental program consists of seven reinforced concrete ferrocement beams. All beams were cross section of: 150 mm, 150 mm and 1600 mm in width, depth and effective span length of the beam respectively, with total length of 1900 mm. The specimens were tested under two point-load loading with 650 mm shear span and 300 mm load distance. The specimens were divided into three groups. The first group was the control specimen; the second group was "group 1" with expanded wire mesh, and the third one was "group 2" with welded wire mesh. All the beams were cast and cured for 28 days. The admixture used in this study was Superplasticizer. Concrete dimensions and reinforcement details for beams are shown in Fig. 2. The beams specimens' are summarized in Table 3.

2.4. Test setup

The beams specimens' were tested under two point-load loading on a universal testing machine of maximum capacity of 500ton with 1600 mm effective span length and 650 mm shear span and 300 mm load distance as shown in Fig. 3. Load was affect at 50 ton increments on the specimen. Dial gauges with an accuracy of 0.01 mm were placed in the bottom of the beam at the mid-point to find the deflection. The load was increased until the specimen reached to failure. Load & displacement were recorded.

2.5. Test results and discussion

2.5.1. Ultimate loads

Table 4 shows the ultimate loads of all beams. The ultimate load of control beams B1 is 95.00 KN. The beams from B1-1 to B1-3 had relatively higher ultimate loads than control. The ultimate loads of the expanded wire mesh beams ranged from 112.00 KN to 128.00 KN. It is clear that the reinforcement technique led to increase the ultimate load of the examined beams. Table 5 summarizes the relative ultimate loads of the expanded wire mesh beams. The relative ultimate load ranged from 117.89% to 134.74% depending on the number of layers of expanded wire mesh.

Using three layers led to the highest relative strength value while using one layer led to the lowest relative ultimate load.

As shown in Table 4, the beams from B1-2 to B3-2 had higher ultimate loads also than control. The ultimate loads of the welded wire mesh beams ranged from 111.50 KN to 129.00 KN. It is clear that the reinforcement technique led to increase the ultimate load of the examined beams. Table 4 summarizes the relative ultimate loads of the welded wire mesh beams. The relative ultimate load ranged from 117.37% to 135.79% depending on the number of layers of welded wire mesh. Using three layers led to the highest relative strength value while using one layer led to the lowest relative ultimate load.

The increase of the load carrying capacity of the expanded and welded wire mesh beams is mainly due to increasing the volume fraction.

2.5.2. Ultimate deflection

Table 4 shows the ultimate deflection of all beams. The recorded displacement was decreased with ratio between 4.8% and 12.0% of the deflection at maximum load of the reference beam. For group 1,

Table 2
Ferrocement mortar mix properties.

Mix Design	Cement (kg/m^3)	Sand (kg/m^3)	Water (kg/m^3)	Super plasticizer (kg/m^3)
M	700	1400	245	7

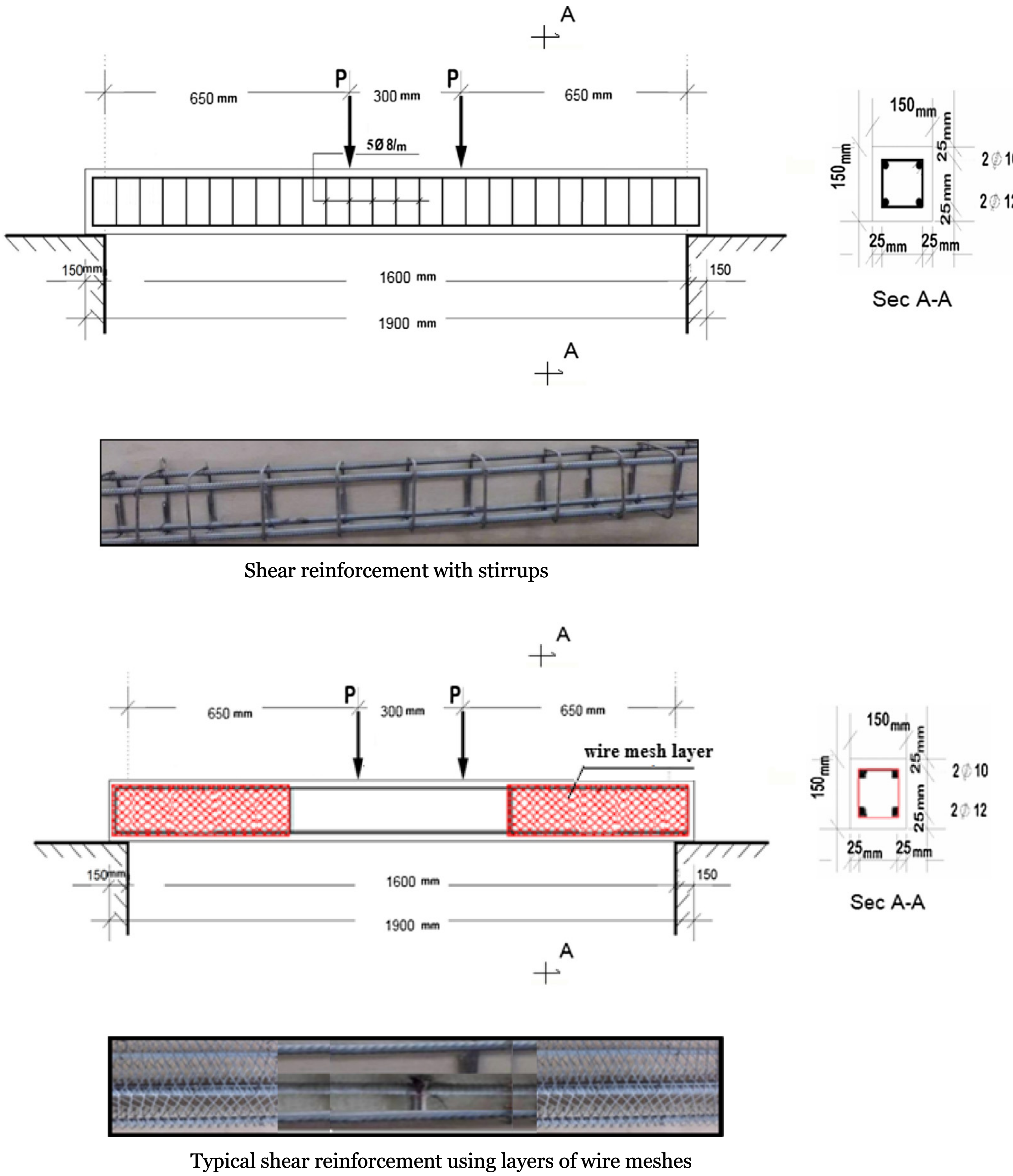

Fig. 2. Beams Geometry and reinforcement detail.

Table 3
Beams specimens' notation.

Series	Specimen No.	Specimens description	Reinf. Tension	Compression	Stirrups
Control	B1	Control specimen	2 φ12	2 φ10	φ6@200
Group 1 "Expanded wire mesh"	B1-1	One layer expanded	2 φ12	2 φ10	–
	B2-1	Two layer expanded	2 φ12	2 φ10	–
	B3-1	Three layer expanded	2 φ12	2 φ10	–
Group 2 "Welded wire mesh"	B1-2	One layer welded	2 φ12	2 φ10	–
	B2-2	Two layer welded	2 φ12	2 φ10	–
	B3-2	Three layer welded	2 φ12	2 φ10	–

the deflection for B1-1 was 1.19 mm with respect to 1.25 mm for the reference specimen with a ratio of 95.20%. For B2-1 the deflection was 1.15 mm which decreased than the previous specimen B1-1 due to using two layers of expanded wire mesh in reinforcement. B3-1 recorded the lowest deflection which equals to 1.10 mm with a ratio of 88.00% with respect to the reference beam. This is due to the presence of three layers of expanded wire mesh.

The deflection of beams of group 2 recorded slightly higher values of deflection for group 1. For B1-2 the deflection recorded 1.20 mm with respect to 1.25 mm for reference beam with a ratio of 96.00%. B2-2 and B3-2 recorded 1.17 mm and 1.12 mm with a ratio of 93.60% and 89.60% respectively. Finally, there is a reduction in deflection for groups 1 & 2 with respect to the reference beam.

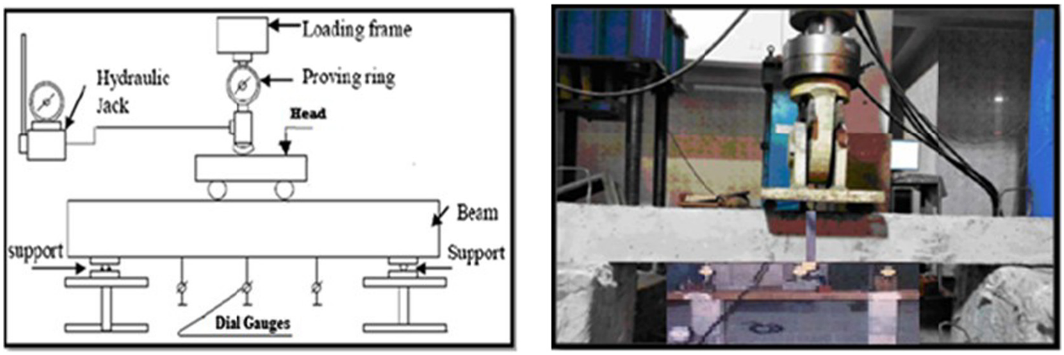

Fig. 3. Test setup.

Table 4
Experimental test results.

Se-ries	Beam-Specimen	Failure Load $P_{ult.}$(KN)	Max. midspan deflection $\Delta_{ult.}$(mm)	Max. Shear Stress V_u (MPa)	Stiff-Ness (KN/mm)	Toughness (KN·mm)
Control	B1	95.0	1.25	2.43	72.55	59.40
Group 1	B1-1	112.0	1.19	2.87	76.25	86.80
	B2-1	115.0	1.15	2.95	78.95	88.70
	B3-1	128.0	1.10	3.28	80.01	94.50
Group 2	B1-2	111.5	1.20	2.95	89.72	88.10
	B2-2	123.0	1.17	3.15	100.38	100.90
	B3-2	129.0	1.12	3.31	107.52	119.30

Table 5
Relative values of experimental test results.

Series	Beam – Specimen	$P_{ult.}/P_{ult.ref.}$ (%)	$\Delta_{ult.}/\Delta_{ult..ref.}$ (%)	V_u/V_u(%)	Stiff./Stiff.$_{ref.}$ (%)	Tough./Tough.$_{ref.}$ (%)
Control	B1	100.00	100.00	100.00	100.00	100.00
Group 1	B1-1	117.89	95.20	118.11	105.10	146.13
	B2-1	121.05	92.20	121.40	108.82	149.33
	B3-1	134.74	88.00	134.98	110.28	159.09
Group 2	B1-2	117.37	96.00	121.40	123.68	148.32
	B2-2	129.47	93.60	129.63	138.36	169.87
	B3-2	135.79	89.60	136.21	148.20	184.01

The decrease of the ultimate deflection of the welded and expanded wire mesh beams is mainly due to increasing the volume fraction.

2.5.3. Stiffness

The ability of the reinforced concrete beam to resist cracking can be expressed in terms of its stiffness. Table 4 shows the computed stiffness of all beams. It is calculated as the slope of the straight line of the load–displacement curve. Fig. 4 was used to compute the stiffness of the tested RC beams.

Table 5 summarizes the relative stiffness of the wire mesh beams. The relative stiffness ranged from 105.10% to 148.20% depending on the types of wire mesh and number of layers. Using three layer welded wire mesh led to the highest in relative stiffness value, while using one layer expanded wire mesh led to the lowest relative stiffness due to increasing the volume fraction. The relative stiffness for beams B1-1, B2-1, B3-1, B1-2, B2-2 & B3-2 was 105.10%, 108.82%, 110.28%, 123.68%, 138.36% & 148.20% respectively.

2.5.4. Toughness

It is calculated as the area under the load displacement curve. Fig. 4 was used to calculate the toughness and the results were given in Table 4. The toughness of the wire mesh beams was higher than that calculated for the control beam B1. The toughness of the wire mesh beams ranged from 86.80 KN·mm to 119.30 KN·mm while the toughness of the control beam was 59.40 KN·mm. Table 5 indicated that the relative toughness of the ferrocement beams ranged from 146.13% to 184.01%. It is clear from the results that the enhancement to impact or energy absorption was occurred due to the reinforcement technique from where the types used of wire mesh and number of layers.

2.5.5. Shear stress

For the control specimen B1, the obtained shear stress based on the ECP203/2007[8] Eq. (4)–(14) was 2.43 MPa. For beams B1-1, B2-1 and B3-1 the obtained shear stresses were 2.87 MPa, 2.95 Mpa and 3.28 MPa respectively with an enhancement of 118.11%, 121.40% & 134.98%, whereas the shear stresses were 2.95 MPa, 3.15 Mpa and 3.31 MPa B1-2, B2-2 and B3-2 respectively with an enhancement of 121.40%, 129.63% & 136.21% as shown in Tables 4 and 5.

The increase of the ultimate shear capacity of the welded wire mesh beams when compared with the expanded wire mesh beams is mainly due to increasing the volume of fraction.

3. Analytical study

The analytical study was done to verify the results obtained from the experimental study. A group of seven specimens of reinforced concrete ferrocement beams were modeled and analyzed by

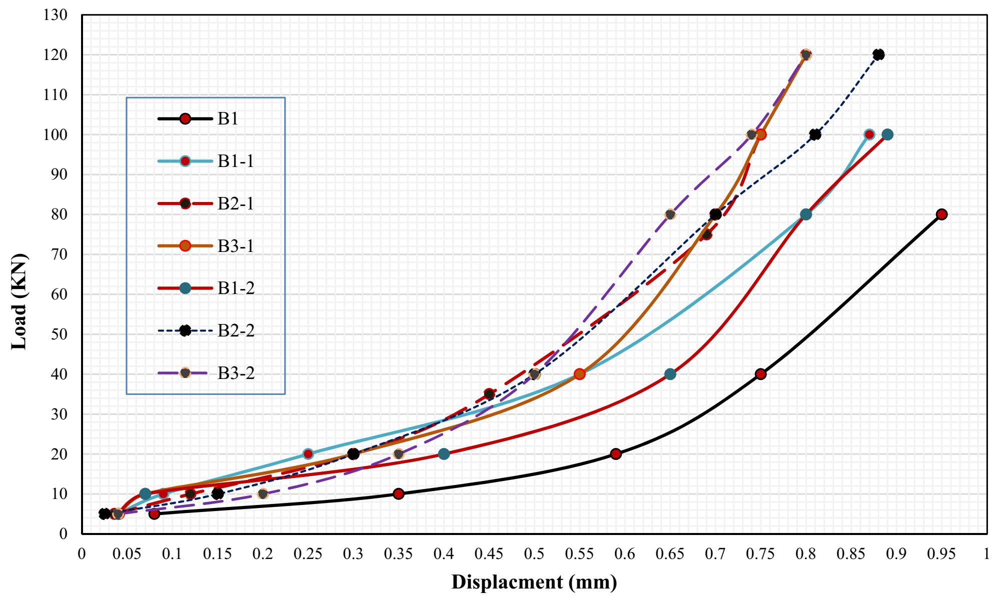

Fig. 4. Load –midspan displacement curves for tested beams.

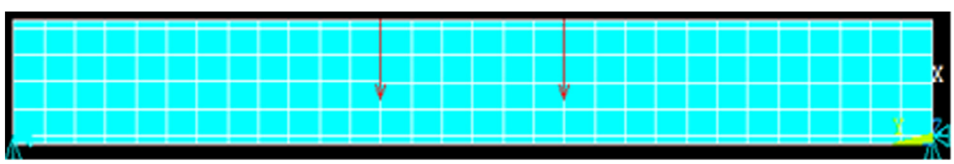

Fig. 5. NLFEA model of examined beams.

using ANSYS [9]. Specimens were 1600 mm span and a cross-section 150 × 150 mm.

3.1. Modeling

Non-linear finite element analysis; (NLFEA) was carried out to investigate the shear performance of ferrocement composite beams specimens employing ANSYS 14.5 Software as indicated in Fig. 5. The investigated behavior includes the cracks pattern, shear stresses and the ultimate carrying capacity of the examined beams.

3.1.1. Element types

In this study, SOLID 65 for the concrete as it is suitable for presentation of compression stress-strain curve for concrete other properties. The main and secondary reinforcing steel bars were modelled using LINK 8 3-D element. Also the other innovative composites materials were represented by calculating its volumetric ratio in concrete element using its special properties. The volumetric ratio refers to the ratio of steel to concrete in the element. ANSYS [9] allows the user to enter three rebar materials in the concrete. Each material corresponds to x, y, and z. The orientation angles refer to the orientation of the reinforcement in the smeared model. Therefore, expanded & welded wire meshes were presented as smeared layers with volumetric ratio as it is referred below. The analytical solution scheme adopted for non-linear analysis was an incremental load procedure. The geometry and node locations for elements type solid65 and link8 are shown in Fig. 6a, 6b respectively.

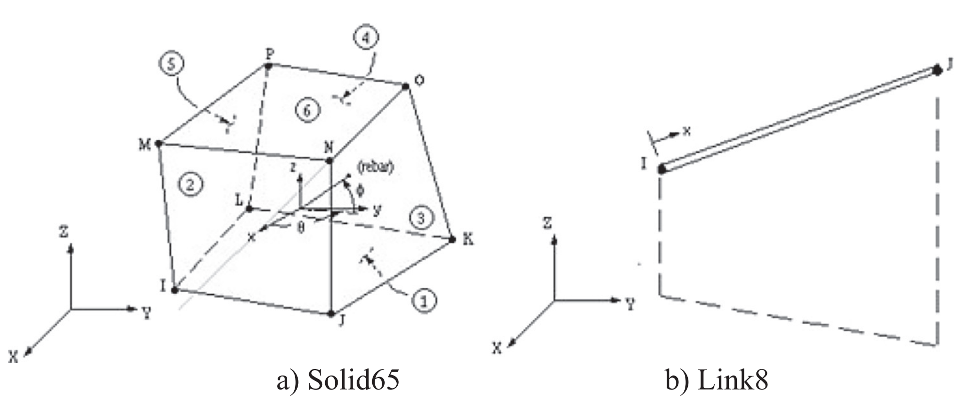

Fig. 6. Geometry and node locations for element types.

3.1.2. Material properties

This part show the material properties for concrete, reinforcing steel bars & reinforcing expanded & welded wire mesh.

- The material properties constants for con-crete are input as follows:

Elastic modulus of elasticity ($E_c = 4400\sqrt{f_{cu}} = 24100\ \text{N/mm}^2$) and Poisson's ratio ($v = 0.3$) [8].

- The other material properties for reinforcing steel are input as follows:
  1. Elastic Modulus of elasticity ($E_s = 200\ \text{k N/mm}^2$)
  2. Yield stress ($f_y = 360\ \text{N/mm}^2$ & $f_{yst} = 240\ \text{N/mm}^2$)
  3. Poisson's ratio ($v = 0.2$)
  4. Area of steel of 2φ12 (As = 226 mm^2)
  5. Area of steel of 2φ10 (As = 157 mm^2)
- The material properties for expanded wire mesh are input as follows:
  1. Yield stress ($f_y = 250\ \text{N/mm}^2$)
  2. The diamond size is 16.5 × 31 mm with thickness of 1.25 mm
  3. Volumetric ratio of one layer of expanded mesh (V1 = 0.0093)
  4. Volumetric ratio of two layer of expanded mesh (V1 = 0.0186)
  5. Volumetric ratio of three layer of expanded mesh (V1 = 0.0279)
- The material properties for welded wire mesh are input as follows:
  1. Yield stress ($f_y = 400\ \text{N/mm}^2$)
  2. The size of opening is 12.5 × 12.5 mm with wires of diameter 0.7 mm
  3. Volumetric ratio of one layer of expanded mesh (V1 = 0.0031)
  4. Volumetric ratio of two layer of expanded mesh (V1 = 0.0062)
  5. Volumetric ratio of three layer of expanded mesh (V1 = 0.0093)

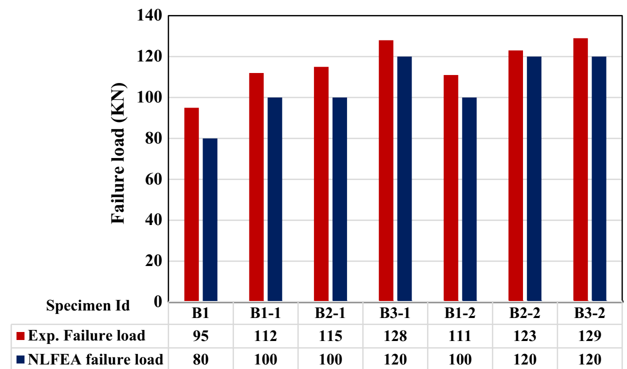

Fig. 7. Comparison between failure load of experimental and NLFE analysis (KN).

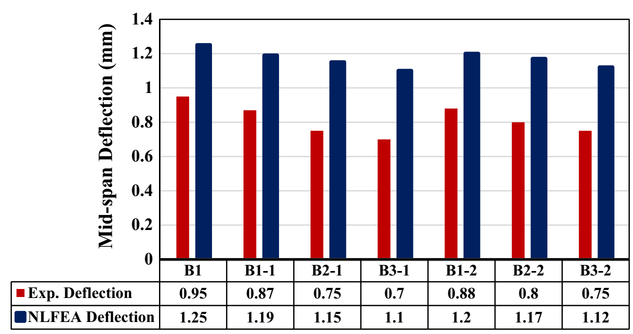

Fig. 8. Comparison between mid-span deflection of experimental and NLFE analysis (mm).

3.2. Analytical results discussion (model verfication)

The finite element analysis of the model in this study examines cracking, yielding of the steel and failure strength of the beam. The nonlinear response is computed by the Newton-Raphson method of analysis. Loading was incrementally increased until un-

Table 6
Analytical results.

Series	Beam-Specimen	Failure Load $P_{ult.}$ (KN)	Max. midspan deflection $\Delta_{ult.}$ (mm)	Max. Shear Stress V_u (MPa)	Stiff-Ness(KN/mm)	Toughness (KN·mm)
Control	B1	80	0.95	2.05	81.63	40.12
Group 1	B1-1	100	0.87	2.56	84.03	59.20
	B2-1	100	0.75	2.56	87.20	68.13
	B3-1	120	0.70	3.07	88.88	70.06
Group 2	B1-2	100	0.88	2.56	91.12	65.06
	B2-2	120	0.80	2.87	117.64	73.18
	B3-2	120	0.75	3.07	123.07	77.86

Table 7
Relative values of analytical results.

Series	Beam – Specimen	$P_{ult.}/P_{ult.ref.}$ (%)	$\Delta_{ult.}/\Delta_{ult..ref.}$ (%)	V_u/V_u(%)	Stiff./Stiff.$_{ref.}$ (%)	Tough./Tough.$_{ref.}$ (%)
Control	B1	100.00	100.00	100.00	100.00	100.00
Group 1	B1-1	125.00	95.58	124.88	102.94	147.56
	B2-1	125.00	78.95	124.88	106.82	169.82
	B3-1	150.00	73.68	149.76	108.88	174.63
Group 2	B1-2	125.00	92.63	124.88	111.63	162.16
	B2-2	150.00	84.21	140.00	144.11	182.40
	B3-2	150.00	78.95	149.76	150.77	194.07

convergence which means failure. The finite element analysis predictions including the ultimate loads, deflection and shear stresses are summarized in Table 6.

3.2.1. Ultimate loads

Table 6 shows the ultimate loads of all beams. The ultimate load of control beams B1 is 80 KN. The beams from B1-1 to B1-3 had relatively higher ultimate loads than control. The ultimate loads of the expanded wire mesh beams ranged from 100 KN to 120 KN. Table 7 summarizes the relative ultimate loads of the expanded wire mesh beams. The relative ultimate load ranged from 125% to 150% depending on the number of layers of expanded wire mesh. Using three layers led to the highest relative strength value while using one layer led to the lowest relative ultimate load.

As shown in Table 6, the beams from B1-2 to B3-2 had higher ultimate loads also than control. The ultimate loads of the welded wire mesh beams ranged from 100 KN to 120 KN. Table 7 summarizes the relative ultimate loads of the welded wire mesh beams.

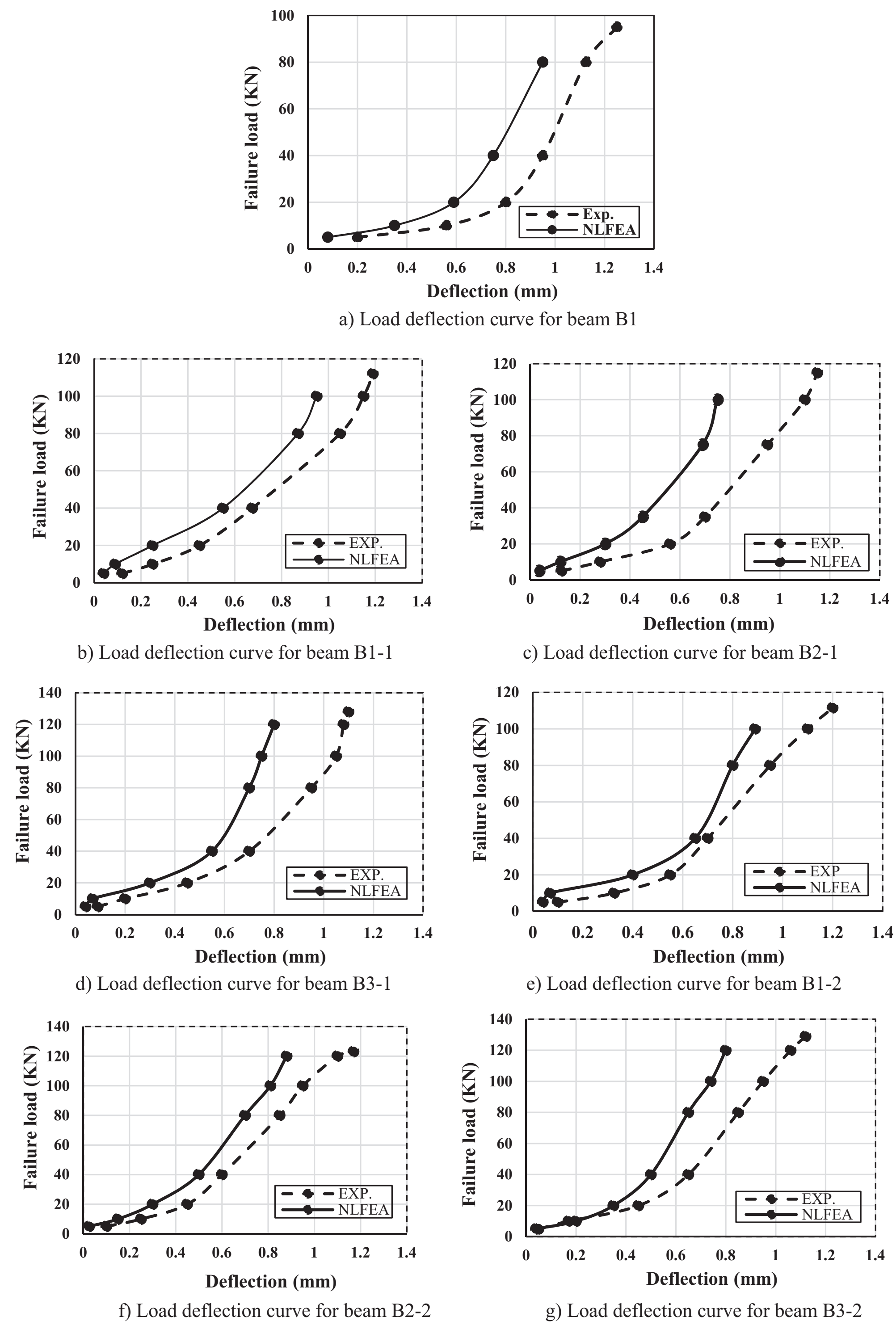

Fig. 9. Comparison of load deflection curves for all specimens.

The relative ultimate load ranged from 125% to 150% depending on the number of layers of welded wire mesh. Using three layers led to the highest relative strength value while using one layer led to the lowest relative ultimate load.

Table 6 shows the ultimate deflection of all beams. For group 1, the deflection for B1-1 was 0.87 mm with respect to 0.95 mm for the reference specimen with a ratio of 95.58%. For B2-1 the deflection was 0.75 mm which decreased than the previous specimen B1-1 due to using two layers of expanded wire mesh in reinforcement. B3-1 recorded the lowest deflection which equals to 0.70 mm with a ratio of 73.68% with respect to the reference beam. This is due to the presence of three layers of expanded wire mesh.

The deflection of beams of group 2 recorded slightly higher values of deflection for group 1. For B1-2 the deflection recorded 0.88 mm with respect to 0.95 mm for reference beam with a ratio of 92.63%. B2-2 and B3-2 recorded 0.80 mm and 0.75 mm with a ratio of 84.21% and 78.95% respectively. Finally, there is a reduction in deflection for groups 1 & 2 with respect to the reference beam Figs. 7 and 8.

3.2.2. Stiffness

Table 6 shows the computed stiffness of all beams. Fig. 9 was used to compute the stiffness of the tested RC beams.

Table 7 summarizes the relative stiffness of the wire mesh beams. The relative stiffness ranged from 102.94% to 150.77% depending on the types of wire mesh and number of layers. Using three layer welded wire mesh led to the highest in relative stiffness value, while using one layer expanded wire mesh led to the lowest relative stiffness due to increasing the volume fraction. The relative stiffness for beams B1-1, B2-1, B3-1, B1-2, B2-2 & B3-2 was 102.94%, 106.82%, 108.88%, 111.63%, 144.11% & 150.77% respectively.

3.2.3. Toughness

Fig. 9 was used to calculate the toughness and the results were given in Table 6. The toughness of the wire mesh beams was higher than that calculated for the control beam B1. The toughness of the wire mesh beams ranged from 59.20 KN·mm to 77.86 KN·mm while the toughness of the control beam was 40.12 KN·mm. Table 7 indicated that the relative toughness of the ferrocement beams ranged from 147.56% to 194.07% as shown in Tables 6 and 7.

3.2.4. Shear stress

As shown in Fig. 12 the control specimen B1, the obtained shear stress was 2.43 MPa. For beams B1-1, B2-1 and B3-1 the obtained shear stresses were 2.87 MPa, 2.95 Mpa and 3.28 MPa respectively with an enhancement of 118.11%, 121.40% & 134.98%, whereas the shear stresses were 2.95 MPa, 3.15 Mpa and 3.31 MPa B1-2, B2-2 and B3-2 respectively with an enhancement of 121.40%, 129.63% & 136.21% as shown in Tables 6 and 7.

4. Comparison between experimental results and NLFEA results

The goal of the comparison of experimental and non-linear results is to ensure that NLFE models are suitable to exhibit the behavior response of the ferrocement beams.

The seven analytical models were compared with the experimental results in terms of ultimate load, ultimate deflection, shear stress and crack pattern.

4.1. Ultimate load

Table 8 and Fig. 7 showed a fairly agreement between the experimental & NLFEA load capacity where; $Pu_{NLFEA}/Pu_{exp.}$ with a ratio of 0.84 for control. For beams B1-1, B2-1 and B3-1 $Pu_{NLFEA}/Pu_{exp.}$ ratios were 0.89, 0.87 and 0.93 respectively. For beams B1-2, B2-2 and B3-2 $Pu_{NLFEA}/Pu_{exp.}$ ratios were 0.90, 0.97 and 0.93 respectively.

The NLFE analysis showed the object of test parameters considered on the load carrying capacity.

4.2. Ultimate deflection

Fig. 8 showed comparison between deflection from experimental test & NLFEA. Fig. 9 showed the load displacement curves for all beams for both experimental and analytical studies. The load

Table 8
Comparison between experimental & NLFE Analysis.

Beam – Specimen	Failure Load Pult. (KN)		Deflection $\Delta_{ult.}$ (mm)		Shear stress V_u (MPa)		$Pu_{NLFEA}/Pu_{exp.}$	$\Delta u_{NLFEA}/\Delta u_{exp.}$	$Vu_{NLFEA}/Vu_{exp.}$
–	NLFEA	EXP	NLFEA	EXP	NLFEA	EXP	–	–	–
B1	80	95.0	0.95	1.25	2.05	2.43	0.84	0.76	0.84
B1-1	100	112.0	0.87	1.19	2.56	2.87	0.89	0.73	0.89
B2-1	100	115.0	0.75	1.15	2.56	2.95	0.87	0.65	0.86
B3-1	120	128.0	0.70	1.10	3.07	3.28	0.93	0.64	0.93
B1-2	100	111.5	0.88	1.20	2.56	2.95	0.90	0.73	0.86
B2-2	120	123.0	0.80	1.17	2.87	3.15	0.97	0.68	0.91
B3-2	120	129.0	0.75	1.12	3.07	3.31	0.93	0.67	0.93

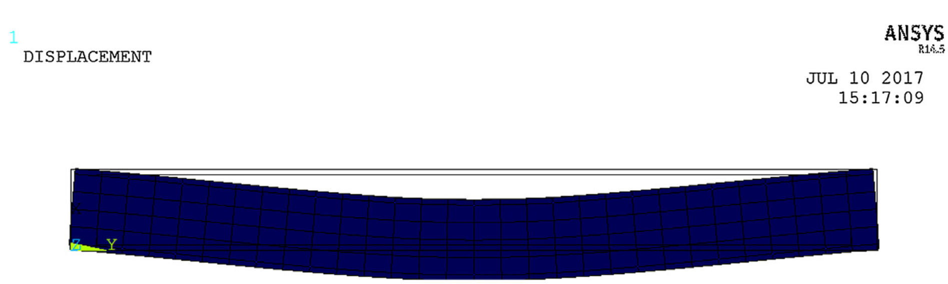

Fig. 10. Typical deformation shape of ferrocement beams.

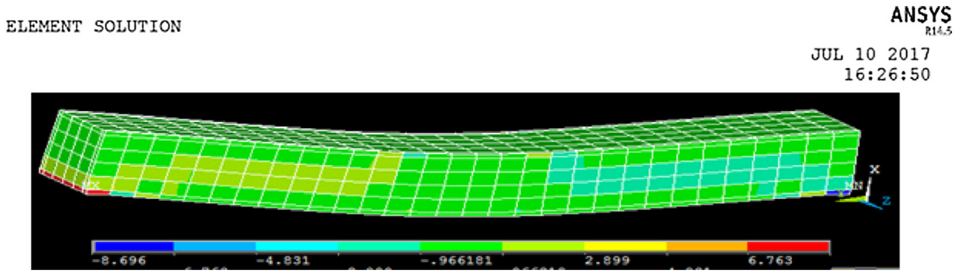

Fig. 11. Typical shear stress diagram in ferrocement beams.

displacement curves for tested specimens and analytical results showed a feasible agreement. Table 8 showed that the beam specimen B1 failed and recorded a deflection ratio $\Delta u_{NLFEA}/\Delta u$ exp. of 0.76. For beams B1-1, B2-1 and B3-1 $\Delta u_{NLFEA}/\Delta u$ exp.ratios were 0.73, 065 and 0.64 respectively. For beams B1-2, B2-2 and B3-2 $\Delta u_{NLFEA}/\Delta u_{exp}$ ratios were 0.73, 0.68 and 0.67 respectively.

The analytical models provided an acceptable load deflection response.

Fig. 10 showed the typical deformed shape of ferrocement beams.

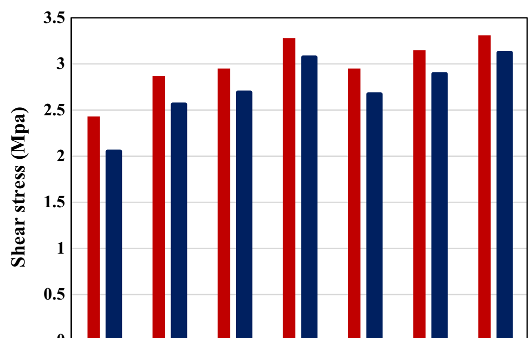

	B1	B1-1	B2-1	B3-1	B1-2	B2-2	B3-2
Exp. Shear stress	2.43	2.87	2.95	3.28	2.95	3.15	3.31
NLFEA Shear stress	2.05	2.56	2.69	3.07	2.67	2.89	3.12

Fig. 12. Comparison between shear stresses of experimental and NLFE analysis (MPa).

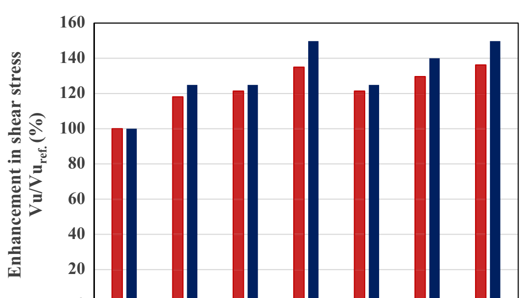

	B1	B1-1	B2-1	B3-1	B1-2	B2-2	B3-2
Vu exp./Vu ref. exp.	100.00	118.11	121.40	134.98	121.40	129.63	136.21
Vu NLFEA/Vu ref. NLFEA	100.00	124.88	124.88	149.76	124.88	140.00	149.76

Fig. 13. Enhancement in shear stress ($Vu/Vu_{ref.}$)%.

4.3. Shear stress

While the main object of this study was to study the effect of using wire mesh reinforcement on shear stress capacity.

As shown in Table 8 the control specimen B1, the obtained shear stress ratio between analytical and experimental shear stress was $Vu_{NLFEA}/Vu_{exp.}$ 0.84. For beams B1-1, B2-1 and B3-1 $Vu_{NLFEA}/Vu_{exp.}$ ratio was 0.89, 0.86 and 0.93 respectively. For beams B1-2, B2-2 and B3-2 $Vu_{NLFEA}/Vu_{exp.}$ ratio was 0.86, 0.91 and 0.93 respectively.

So, The NLFE analysis presented an accurate prediction of ultimate shear stress of experimental specimens.

Fig. 11 showed the typical shear stress diagram of ferrocement beams.

The experimental and analytical study showed a reasonable agreement in shear stress capacity as in Fig. 12.

Fig. 13 showed the enhancement in shear stress for experimental to analytical models.

4.4. Cracks pattern

Fig. 14 indicate comparison between crack pattern obtained from experimental test & NLFEA. All beams exhibited similar patterns of crack propagation. These cracks became diagonal and grew toward the loading points.

4.5. Mode of failure

Fig. 15 showed the mode of failure for ferrocement beams which was shear compression failure.

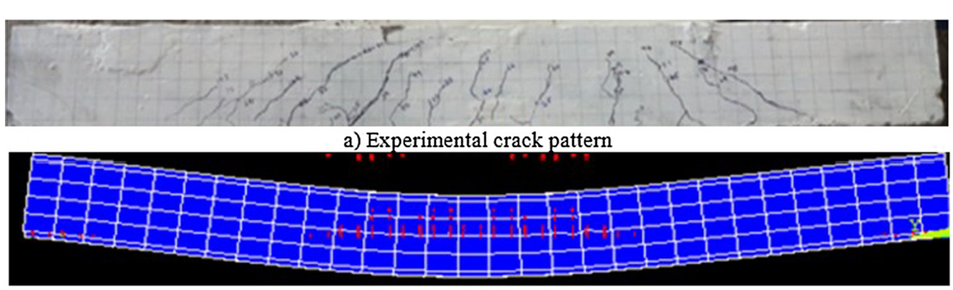

a) Experimental crack pattern

b) NLFEA crack pattern

Fig. 14. Crack pattern of wire mesh beams.

Fig. 15. Modes of failure for ferrocement beams (Shear compression failure).

5. Conclusions

The main conclusions can be summarized as follows:

1. Welded and expanded wire meshes show multiple features over steel reinforcement, especially for structures with complex shapes and curvatures, because they are lighter, easier to handle, easier to cut, and easier to bend than steel reinforcement.
2. Ferrocement concrete specimens reinforced by expanded or welded steel wire mesh exhibit superior ultimate loads compared to the control ones under flexural loadings.
3. Welded wire mesh contributed to increase load carrying capacity, deflection shear stresses, stiffness & toughness higher than expanded wire mesh.
4. Increasing the number of layers of expanded and welded wire meshes led to improve Ultimate load, load deflection, stiffness, toughness, and shear stress of ferrocement beams.
5. Cracks with greater number and narrower widths were observed for those beams re-inforced with steel meshes compared with beams reinforced with steel reinforcement.
6. Accepted agreement between experimental results and analytical ones. Therefore experimental program was carried out and can be helpful for further parametric studies including various parameters could be investigated.
7. The presented work gives good prediction of shear strength of ferrocement beams where the average ratio ($Vu_{NLFEA}/Vu_{\exp}$) was found to be 0.90.

Finally, using ferrocement composite in shear reinforcement has good effectiveness for increasing the shear capacity for concrete beams, cracks behavior, deflection and load carrying capacity.

Conflict of interest

None.

Acknowledgements

The authors wish to acknowledge the Spiritual support of the Civil Engineering Department, Faculty of Engineering Shoubra, Benha University, Cairo, Egypt.

References

[1] ACI Committee 549, State of the art report on ferrocement. ACI 549-R97 manual of concrete practice, Detroit, 1997.
[2] ACI Committee 549-1R-88. Guide for design construction and repair of ferrocement. ACI 549-1R-88 and 1R-93 manual of concrete practice, Detroit, 1993.
[3] G.J. Al-Sulaimani, S.F. Ahmad, I.A. Basunbul, Study of the flexural strength of ferrocement ‘flanged’ beams, Arabian J. Sci. Eng. 14 (1) (1989) 33–46.
[4] M.A. Mansur, K.C.G. Ong, Shear strength of ferrocement beams, Am. Concr. Inst. Struct. J. 84 (1) (1987) 10–17.
[5] E.H. Fahmy, Y.B. Shaheen, M.N. Abou Zeid, H. Gaafar, Ferro-Cement Sandwich and Cored Panels for Floor and Wall Construction, in: Proceedings of the 29th Conference on Our World in Concrete and Structures, 2004, pp. 245–252.
[6] P.J. Walker, M. Damo, Shear Reinforcement for Brickwork Beams Using Ferrocement, J. Ferrocement, 27 (1) (1997).
[7] I.A. Basunbul, A.A. Gubati, G.J. Al-Sulaimani, M.H. Baluch, Flexural Behavior of Ferro-Cement Sand-Wish Load Bearing wall Panel, ACI Mater. J. 87 (4) (1991) 348–354.
[8] E.C.P. 203, Egyptian Code of Practice: Design and Construction for Reinforced Concrete Structures, Egypt Cairo, 2007.
[9] ANSYS, “Engineering Analysis system user’s Manual” 2005, vol. 1&2, and theoretical manual. Revision 8.0, Swanson analysis system inc., Houston, Pennsylvania.